Available online at www.sciencedirect.com
SCIENCE DIRECT®
International Journal of Mass Spectrometry 227 (2003) 453–469
International Journal of Mass Spectrometry
www.elsevier.com/locate/ijms

Tautomerization and dissociation of ethylene phosphonate ions $[–OCH_2CH_2O–]P(H)=O^{\bullet+}$: an experimental and CBS-QB3 computational study

Lisa N. Heydorn[a], Peter C. Burgers[b], Paul J.A. Ruttink[c], Johan K. Terlouw[a,*]

[a] *Department of Chemistry, McMaster University, Hamilton, Ont., Canada L8S 4M1*
[b] *Hercules European Research Center BV, Nijverheidsweg 60, 3771 ME Barneveld, The Netherlands*
[c] *Theoretical Chemistry Group, Department of Chemistry, University of Utrecht, 3584 CH Utrecht, The Netherlands*

Received 4 March 2002; accepted 31 July 2002

Abstract

The unimolecular gas-phase chemistry of the cyclic title ion, $[–OCH_2CH_2O–]P(H)=O^{\bullet+}$, **1a**$^{\bullet+}$, and its tautomer ethylene phosphite, $[–OCH_2CH_2O–]P–OH^{\bullet+}$, **1b**$^{\bullet+}$, was investigated using mass spectrometry-based experiments in conjunction with isotopic labelling and computational quantum chemistry, at the CBS-QB3 level of theory. A facile tautomerization of the "keto" ion **1a**$^{\bullet+}$ into its more stable (by 34 kcal/mol) "enol" isomer **1b**$^{\bullet+}$ is prevented by a substantial 1,2-H shift barrier (14 kcal/mol relative to **1a**$^{\bullet+}$). In line with this, the collision-induced dissociation (CID) and neutralization-reionization (NR) spectra of the two isomers are characteristically different. Unlike the corresponding acyclic dimethyl phosphonate/phosphite tautomers, $(CH_3O)_2P(H)=O^{\bullet+}/(CH_3O)_2P–OH^{\bullet+}$, where the phosphonate isomer rapidly loses its structure identity by a facile distonicization into $CH_2O–(CH_3O)P(H)OH^{\bullet+}$, the barrier for this reaction in **1a**$^{\bullet+}$ is prohibitively high and the cyclic distonic 1,2-H shift isomer $[–OCH_2CH_2O(H)–]P=O^{\bullet+}$, **1c**$^{\bullet+}$, is not directly accessible.

The 1,2-H shift barrier separating **1a**$^{\bullet+}$ and **1b**$^{\bullet+}$ is calculated to lie close to the thermochemical threshold for the formation of $C_2H_4{}^{\bullet+}$ + HO–P(=O)$_2$. This reaction dominates the closely similar metastable ion (MI) spectra of these tautomers. At these elevated energies, the "enol" ion **1b**$^{\bullet+}$ can undergo ring-opening by CH_2–O or CH_2–CH_2 cleavage, yielding ion–dipole complexes of the type $[C_2H_4]^{\bullet+}$/HO–P(=O)$_2$, **1e**$^{\bullet+}$, and H-bridged radical cations CH_2=O···[H–O–P–OCH_2]$^{\bullet+}$, **1f**$^{\bullet+}$, respectively. Moreover, communication of **1b**$^{\bullet+}$ with the distonic ion **1c**$^{\bullet+}$ now also becomes feasible. These computational findings account for the similarity of the MI spectra and provide a rationale for the observation that in the losses of CO, $HCO^{\bullet}$ and $C_2H_3O^{\bullet}$ from metastable ions $[–OCH_2CH_2O–]P(H)={}^{18}O^{\bullet+}$ and $[–OCH_2CH_2O–]P–{}^{18}OH^{\bullet+}$, the ^{18}O-atom loses its positional identity.

Theory and experiment yield a consistent potential energy profile for the cyclic phosphonate/phosphite system showing that non-dissociating ions **1a**$^{\bullet+}$ retain their structure identity in the microsecond time-frame. However, the interaction of **1a** with a benzonitrile (BN) molecule in a chemical ionization type experiment readily yields the more stable "enol" type ion **1b**$^{\bullet+}$. Experiments with benzonitrile-d_5 support the proposal that this interaction does not involve the lowering of the 1,2-H

* Corresponding author. Tel.: +1-905-525-9140x23490; fax: +1-905-525-2509.
E-mail address: terlouwj@mcmaster.ca (J.K. Terlouw).

1387-3806/03/$ – see front matter
doi:10.1016/S1387-3806(03)00106-4

shift barrier between the tautomers, via a proton-transport catalysis type mechanism. Rather, a “quid-pro-quo” mechanism is operative, analogous to that proposed for the benzonitrile-assisted enolization of acetamide [Int. J. Mass Spectrom. 210/211 (2001) 489].

Keywords: Phosphonate/phosphite tautomerism; Catalysis; Tandem mass spectrometry; Ab initio calculations; CBS-QB3; 1,3,2-Dioxaphospholane; 2-Oxide; Quid-pro-quo

1. Introduction

Gas-phase phosphorus ion chemistry is intimately related to solution phosphorus chemistry [1] and an incentive for its study derives from the intrinsic and practical importance of phosphorus compounds [2,3] and from the significant role of mass spectrometry in their characterization as pesticides, drugs, and endogenous toxic agents (selected reviews: [4]).

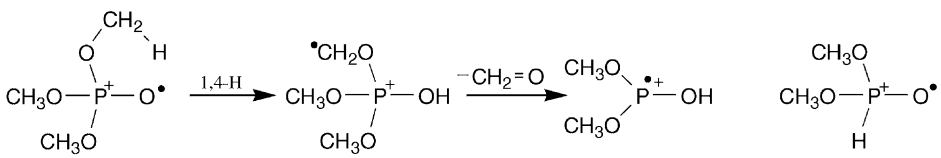

TMP$^{\bullet+}$ $\mathbf{a_2}^{\bullet+}$ $\mathbf{a_1}^{\bullet+}$

One class of compounds that has attracted a great deal of interest [5] are organophosphorus esters which are widely used as pesticides. The conventional electron impact mass spectra of alkyl and aryl phosphates and phosphites were already studied when organic mass spectrometry was still in its infancy [6]. Renewed interest in the gas-phase ion chemistry of these esters started in the mid-eighties when tandem mass spectrometry (MS/MS) [7] using both high- and low-energy collision-induced dissociation (CID) experiments [8] on magnetic deflection, quadrupole, Fourier transform ion cyclotron resonance (FT-ICR) and ion trap mass spectrometers became available to probe the structure of stable and isomerizing ions [9]. One important highlight of the seminal studies of the Purdue groups of Cooks and Kenttämaa [10] is that the long-lived radical cations of simple organophosphates isomerize spontaneously to more stable distonic ions (ions with formally separate radical and charge sites) [10b,11]. The computational finding that a localized radical centre is present at the *oxo* oxygen atom of the initially generated molecular ion may provide a chemical rationalization for this behaviour [12].

A case in point is the behaviour of trimethyl phosphate (TMP) which upon electron impact rearranges into the distonic ion depicted as below and whose lowest energy dissociation route, loss of CH_2=O, yields the radical cation of dimethyl phosphite, $\mathbf{a_2}^{\bullet+}$.

Ion $\mathbf{a_2}^{\bullet+}$ represents the “enol” tautomer of the “keto” ion $\mathbf{a_1}^{\bullet+}$, ionized dimethyl phosphonate (DMP). Its neutral counterpart, $\mathbf{a_2}$, is less stable than the phosphonate, $\mathbf{a_1}$, by 15 kcal/mol and in the condensed phase, the phosphite intermolecularly rearranges into the phosphonate. However, upon ionization, the stability order reverses and $\mathbf{a_2}^{\bullet+}$ is more stable than $\mathbf{a_1}^{\bullet+}$, by 31 kcal/mol [13].

Tautomerization in simple organic radical cations and their neutral counterparts is of fundamental importance and has therefore been studied in great detail, particularly for keto-to-enol isomerization reactions [14]. In this context, proton-transport catalysis in ion–molecule encounter complexes, that is the phenomenon that the neutral promotes the tautomerization of the ionic component of the complex, has recently received a great deal of attention both from theory and experiment (for selected references see [15]). One interesting example is the benzonitrile-assisted enolization of ionized acetone [16]. Enolization of

the acetone radical cation into its more stable isomer CH_2=C(OH)$CH_3^{\bullet+}$ does not occur unassisted because the associated 1,3-H shift imposes a high barrier. However, benzonitrile (BN) has a proton affinity which is higher than that of the CH_2 and equal to that of the O in the $CH_2C(O)CH_3^{\bullet}$ radical and it successfully catalyzes the enolization. Benzonitrile also catalyzes the enolization of acetamide, but here a different mechanism is operative [17].

In line with the above, both the spontaneous and the benzonitrile-assisted tautomerization of DMP has recently been studied in considerable detail by a variety of experimental methods and computational chemistry at the CBS-QB3 level of theory [13], see below.

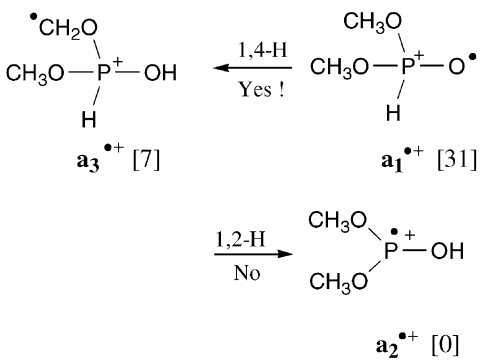

It was concluded that in the microsecond time-frame DMP ions $\mathbf{a_1}^{\bullet+}$ have completely isomerized into the very stable distonic ions $\mathbf{a_3}^{\bullet+}$ by way of a 1,4-H shift. Experiments clearly show that further isomerization of $\mathbf{a_3}^{\bullet+}$ into the even more stable enol ions $\mathbf{a_2}^{\bullet+}$ via a 1,3-H shift does not take effect. However, this latter reaction can be induced to occur by interaction of $\mathbf{a_1}^{\bullet+}$ with a suitable base molecule such as benzonitrile in a chemical ionization type experiment. Thus, benzonitrile effectively catalyzes the enolization of DMP ions, not directly via the 1,2-H shift, but via the more circuitous but less energy demanding route $\mathbf{a_1}^{\bullet+} \rightarrow \mathbf{a_3}^{\bullet+} \rightarrow \mathbf{a_2}^{\bullet+}$.

The successful lowering of very large 1,2-H shifts by way of catalysis by a base molecule presents a particularly challenging case [15g]. For example, the very large barrier (~60 kcal/mol) for the 1,2-H shift which separates the pyridine radical cation from its α-ylide isomer can be lowered to a mere 9 kcal/mol by interaction with a judiciously chosen base [15g]. The 1,2-H shift in DMP ions, which has a calculated barrier of 17 kcal/mol, would constitute an even more challenging case in phosphorous containing ions, but as discussed above, an alternative, more economical route is available.

To study direct "keto-to-enol" transformations in phosphorous containing ions, a system should be chosen which cannot undergo facile alternative rearrangements (i.e., 1,3- and 1,4-H shifts) and so we decided to investigate the "keto" and "enol" ions of ethylene phosphonate, i.e., $\mathbf{1a}^{\bullet+}$ and $\mathbf{1b}^{\bullet+}$. In this model system, formation of a distonic ion (i.e. $\mathbf{1c}^{\bullet+}$) is still possible, but only via an undoubtedly energy demanding 1,2-H shift. Thus, in this model system, we should be able to study enolization, both unimolecularly and molecule-assisted.

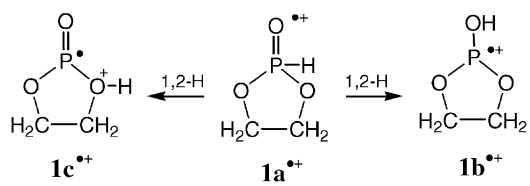

2. Experimental and theoretical methods

2.1. Sample preparation procedures

Ethylene phosphonate (1,3,2-dioxaphospholane, 2-oxide), **1a**, is the parent compound of the class of cyclic phosphonic acid esters which are called cyclic phosphorous acid esters or cyclic hydrogen phosphites in the older literature ([18] and references cited therein). The lower members of this class are highly viscous materials with high boiling points, which are very prone to hydrolysis and difficult to purify. These compounds can be obtained by (i) the reaction of PCl_3 with a given diol, (ii) transesterification of an alkyl phosphonate with 1,2- or 1,3-diols or (iii) hydrolysis, under carefully controlled conditions, of cyclic chlorophosphites [18]. However, with ethylene glycol

as the substrate, the first synthetic route leads, as we have been able to confirm, to highly viscous polymeric products while in the transesterification procedure only the cyclic diethylene diphosphite could be isolated [18a]. Hydrolysis of ethylene chlorophosphite (2-chloro-1,3,2-dioxaphospholane), **I**, with a stoichiometric quantity of water in an inert organic solvent [18c] appeared to be a more profitable route:

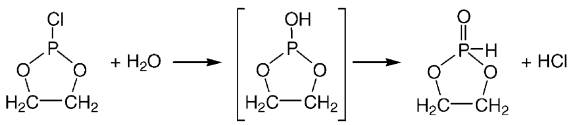

I **1b** **1a**

We have adapted this synthesis to the milligram scale and further modified it by performing the reaction in the presence of an acid-binding agent, pyridine or picoline. Optimal results were obtained by using stoichiometric quantities of all three components, and working under vacuum at low temperatures. In a typical experiment, 200 μL of ethylene chlorophosphite (Aldrich) was transferred to a small glass bulb and frozen (using liquid N_2). Next, the H_2O/pyridine mixture was added and quickly frozen on top of the still frozen chlorophosphite layer. The bulb was then immediately evacuated using a rotary pump and while pumping continuously the two layers were allowed to gradually come to room temperature over a period of 1.5 h, using dry ice as the cooling agent. In this manner, a clear viscous liquid is obtained in which a white precipitate of the pyridine or picoline hydrochloride is suspended. The hydrochloride could be removed by prolonged pumping (∼7 h) at 50 °C with a diffusion pump. The resulting ethylene phosphonate is a clear, colourless, viscous oil, which gave the clean mass spectrum of Fig. 2a. A 1:1 mixture of the phosphonate with its ^{18}O-labelled isotopologue, **1a** (^{18}O) [–OCH_2CH_2O–]P(H)–^{18}O was obtained from 50% ^{18}O-enriched water (Ventron GmbH, Karlsruhe). The isotopologue **1a** (P–D), [–OCH_2CH_2O–]P(D)=O, was prepared in the same way using D_2O.

Ethyl ethylene phosphite, **II**, is a high boiling liquid, stable to distillation and to storage in the absence of moisture and air [18b]. Samples of the unlabelled compound as well as the ^{18}O- and D-labelled isotopologues [–OCH_2CH_2O–]P–$^{18}OC_2H_5$ and [–OCH_2CH_2O–]P–OC_2D_5 were prepared by essentially the same procedure as described above for **1a**, replacing water by a slight excess of (the appropriately labelled) ethanol. No attempts were made to remove the precipitated hydrochloride from the sample as it did not interfere with the experiments.

Methyl ethylene phosphate, **III**, is a well characterized liquid at room temperature whose rapid hydrolysis has been studied in considerable detail ([19] and references cited therein). Samples of the unlabelled compound as well as ^{13}C- and D-labelled isotopologues [–OCH_2CH_2O–]P(=O)O*CH_3 and [–OCH_2CH_2O–]P(=O)OCD_3 were prepared by the methanolysis of 2-chloro-1,3,2-dioxaphospholane-2-oxide (Aldrich) with stoichiometric quantities of the (appropriately labelled) alcohol and picoline, using the procedure described above. Here too, no attempts were made to remove the suspended picoline hydrochloride from the sample.

The benzonitrile and benzonitrile-d_5 samples used in the ion–molecule experiments were of research grade and obtained from Aldrich and C/D/N Isotopes Inc., respectively.

2.2. Tandem mass spectrometry

The tandem mass spectrometry-based experiments were performed with the McMaster University ZAB-R mass spectrometer, a three-sector BE_1E_2 (B: magnetic sector, E: electric sector) type instrument [20]. The instrument is equipped with four collision gas chambers of which the two located in the second field free region (2ffr, in front of E_1) were used for the neutralization-reionization (NR) experiments (for a recent review see: [21]).

The compounds were introduced into the ion source (kept at 100 °C) via a wide-bore all-quartz direct insertion probe connected via an o-ring with a small glass bulb that contains the sample. Ions generated in the source by either electron ionization (EI) or ion–molecule reactions under conditions of chemical ionization (CI), were accelerated to 8 or 10 keV prior

to recording their spontaneous or collision-induced dissociations in the second or the third field free regions as metastable ion (MI) or CID spectra, respectively. The structure of a given product ion in a 2ffr MI or CID spectrum was probed by selectively transmitting the ion by E_1 to a collision chamber in the 3ffr pressurized with O_2 and mass-analyzing its ionic dissociation products by scanning E_2. The resulting MS/MS/MS type spectra are denoted as MI/CID and CID/CID spectra, respectively. All the (high energy) collision experiments were performed at a main beam transmittance (∼70%) such that the probability for multiple collisions is negligible.

For neutralization-reionization mass spectra (NRMS) [21] 8 or 10 keV ions, $m^{\bullet+}$ are selectively transmitted by B to the 2ffr where, in the first collision chamber, charge-exchange neutralization occurs with *N*,*N*-dimethyl aniline (NDMA): $m^{\bullet+}$ (8 or 10 keV) + NDMA → m (8 or 10 keV) + $NDMA^{\bullet+}$. The unreacted ions are deflected away and the remaining fast neutrals are reionized with O_2 in the second collision cell. Scanning E_1 yields the spectrum of the reionized neutrals $m^{\bullet+}$, the "survivor" ions, and their (structure characteristic) charged dissociation products.

All spectra were recorded using a small PC-based data system developed by Mommers Technologies Inc. (Ottawa).

2.3. Computational procedures

The calculations were performed using Gaussian 98 revision A.9 [22] and GAMESS-UK [23]. The standard CBS-QB3 model chemistry [24] was used to probe structures and energies of the key isomeric ions, connecting transition states and dissociation products associated with the ethylene phosphonate/phosphite $C_2H_5O_3P^{\bullet+}$ potential energy surface. The energetic results are presented in Table 1a (equilibrium and transition state energies), Table 1b (dissociation limits) and Scheme 3 while detailed geometries of selected species are displayed in Fig. 1 (the complete set of geometries is available upon request). Frequency calculations gave the correct number of negative eigenvalues for all minima and transition states and the spin contamination was within the acceptable range. The connections of the transition states have been checked by geometry optimizations and frequency calculations.

Table 1a
CBS-QB3 derived energies for the main isomerization reactions of the ethylene phosphonate ion, **1a**$^{\bullet+}$

		E_{total}[a] (B3LYP/CBSB7), Hartree	$E_{total\ (0\ K)}$ (CBS-QB3), Hartree	$E_{rel\ (298\ K)}$ (CBS-QB3), kcal/mol
$CH_2{=}CH_2^{\bullet+}$ + $HOP(=O)_2$	*m/z* 28	−645.93450	−645.06053	0
$[–OCH_2CH_2O–]P(H)=O^{\bullet+}$	**1a**$^{\bullet+}$	−645.95227	−645.08210	−15.0
$[–OCH_2CH_2O–]P–OH^{\bullet+}$	**1b**$^{\bullet+}$	−645.99849	−645.13727	−49.0
$[–OCH_2CH_2O(H)–]P=O^{\bullet+}$	**1c**$^{\bullet+}$	−645.96969	−645.09858	−25.0
$HOCH_2CH_2O–P=O^{\bullet+}$	**1d**$^{\bullet+}$	−645.95824	−645.07099	−7.5
$[CH_2–CH_2–O–P(=O)OH]^{\bullet+}$	**1e**$^{\bullet+}$ (α)	−645.97067	−645.09780	−23.5
$[CH_2–CH_2–O–P(=O)OH]^{+}$	**1e**$^{+}$ (β)	−645.96927	−645.09516	−21.5
$[CH_2O–P–OH]^{\bullet+}\cdots O=CH_2$	**1f**$^{\bullet+}$	−645.97574	−645.08440	−17.5
$CH_3–O–P(=O)OCH_3^{\bullet+}$	**1g**$^{\bullet+}$	−645.96195	−645.08494	−15.0
TS **1a**$^{\bullet+}$ → **1b**$^{\bullet+}$		−645.92174	−645.05956	−0.5
TS **1a**$^{\bullet+}$ → **1c**$^{\bullet+}$		−645.90047	−645.03147	17.0
TS **1c**$^{\bullet+}$ → **1b**$^{\bullet+}$		−645.92366	−645.05914	−1.0
TS **1d**$^{\bullet+}$ → **1c**$^{\bullet+}$		−645.94200	−645.05672	1.4
TS **1b**$^{\bullet+}$ → **1e**$^{\bullet+}$ (α)		−645.94821	−645.06988	−6.5
TS **1e**$^{\bullet+}$ (β) → **1e**$^{\bullet+}$ (α)		−645.96665	−645.09202	−20.0
TS **1e**$^{\bullet+}$ (β) → **1c**$^{\bullet+}$		−645.93931	−645.05951	−0.5
TS **1b**$^{\bullet+}$ → **1f**$^{\bullet+}$		−645.95269	−645.07262	−8.0

[a] The B3LYP energies include ZPVE contributions, scaled by 0.99.

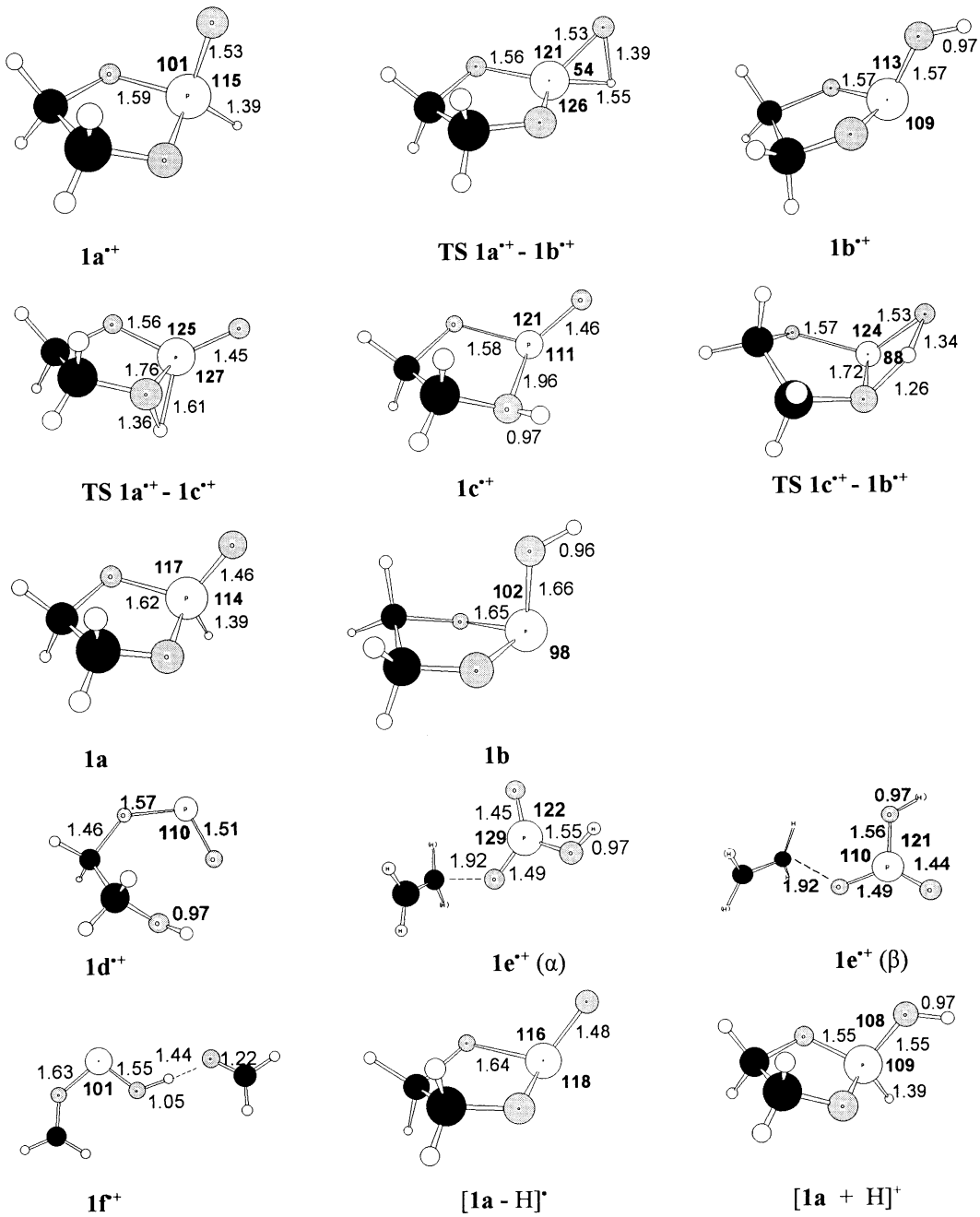

Fig. 1. Optimized geometries of selected ions and neutrals of the ethylene phosphate system. The bond lengths (Å) and angles are presented in normal and bold font, respectively.

Table 1b
Auxiliary energetic information for the ethylene phosphonate system derived from CBS-QB3 calculations

		E_{total} (0 K), Hartree	ΔH_f° (0 K), kcal/mol	ΔH_f° (298 K), kcal/mol
$[–OCH_2CH_2O–]P(H)=O^{\bullet+}$	**1a**$^{\bullet+}$	−645.08210	77.3	71.7
$[–OCH_2CH_2O–]P(H)=O$	**1a**	−645.47424	−168.7	−174.5
$[–OCH_2CH_2O–]P–OH^{\bullet+}$	**1b**$^{\bullet+}$	−645.13727	42.7	37.6
$[–OCH_2CH_2O–]POH$	**1b**	−645.46323	−161.8	−167.3
$[–OCH_2CH_2O–]P(H)OH^+$	[**1a**+ H]$^+$	−645.79180	−2.7	−9.2
$[–OCH_2CH_2O–]P=O^{\bullet}$	[**1a** − H]$^{\bullet}$	−644.83006	−129.8	−134.6
$[–OCH_2CH_2O–]POCH_2CH_3^{\bullet+}$	**II**$^{\bullet+}$	−723.58963	35.6	27.5
$[–OCH_2CH_2O–]P^+$	*m/z* 91	−569.39617	91.3	87.0
$OH^{\bullet}$		−75.64970	8.8	8.8
$(HO)_2P=O^+$	*m/z* 81	−567.29844	30.1	27.1
$CH_2=CH$		−77.74299	72.7	71.7
$HO–P(=O)_2^{\bullet+}$	*m/z* 80	−566.58274	114.0	112.1
$[–O–O–]P–OH^{\cdot+}$	*m/z* 80	−566.52164	152.3	150.6
$CH_2=CH_2$		−78.41263	15.3	13.2
$CH_3O–P(H)OH^{\bullet+}$	*m/z* 80	−531.91692	94.4	90.3
CO		−113.18197	−27.7	−26.9
$CH_3O–P–OH^+$	*m/z* 79	−531.36681	74.4	70.7
$CH_3O(H)–P=O^+$	*m/z* 79	−531.33760	92.7	89.4
$HCO^{\bullet}$		−113.70496	9.4	9.5
$CH_2O–P–OH^{\bullet+}$	*m/z* 78	−530.70506	124.3	121.5
$CH_2=O$		−114.34411	−26.4	−27.3
$HO–P–OH^+$	*m/z* 65	−429.14302	76.4	74.0
$CH_2=CHO^{\cdot}$		−152.93279	4.8	3.0
$CH_2–CHOH^{\bullet+}$	*m/z* 44	−153.22518	186.6	183.9
HO–P=O		−491.85809	−110.0	−111.6
$H–P(=O)_2$		−491.84042	−98.9	−100.6
$CH_2=CH_2^{\bullet+}$	*m/z* 28	−78.02908	258.5	256.5
$HO–P(–O)_2$		−567.03144	−167.6	−169.9
[–O–O–]P–OH		−566.90217	−86.5	−88.5
[–O–O–]P(H)=O		−566.90065	−85.5	−87.9

From a recent validation study [13], it appears that the CBS-QB3 method accurately reproduces the heats of formation of species comprised of a second row element (S or P) bonded to a highly electronegative element. While the computational cost for the present system is fairly high, the CBS-QB3 model chemistry does seem to outperform the comparably expensive G3 method.

3. Results and discussion

3.1. Formation and identification of the "keto and "enol" ions **1a**$^{\bullet+}$ *and* **1b**$^{\bullet+}$

Ions **1a**$^{\bullet+}$ were obtained by electron ionization of ethylene phosphonate and the resulting 70 eV EI mass spectrum is presented in Fig. 2a and b. This spectrum displays a moderately intense molecular ion and principal fragment ions at *m/z* 78 (loss of CH_2O) and *m/z* 28 ($C_2H_4^{\bullet+}$, loss of HPO_3). These two reactions also dominate the CID spectrum of the molecular ion, which is shown in Fig. 3. As will be discussed elsewhere [25], most of the *m/z* 78 ions do not have the $CH_2O–P(H)=O^{\bullet+}$ connectivity expected from CH_2O elimination from the unrearranged molecular ion, **1a**$^{\bullet+}$. Instead, prior to loss of CH_2O, energy-rich ions **1a**$^{\bullet+}$ undergo a fast 1,2-H shift into the "enol" tautomer **1b**$^{\bullet+}$ to yield the more stable $CH_2O–P–OH^{\bullet+}$ isomer (by 18.5 kcal/mol [25]). Similarly, the formation of $C_2H_4^{\bullet+}$ may also be preceded by the tautomerization **1a**$^{\bullet+}$ → **1b**$^{\bullet+}$ (or alternatively **1a**$^{\bullet+}$ → **1c**$^{\bullet+}$) leading to the loss of

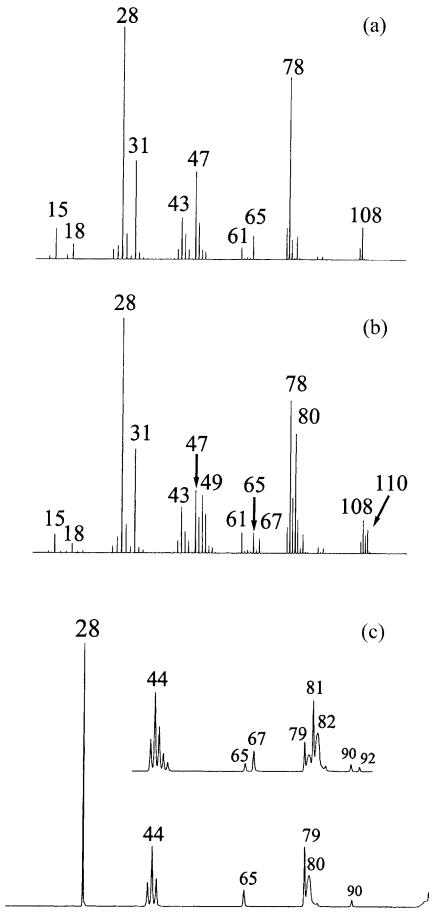

Fig. 2. (a) EI mass spectra of (a) ethylene phosphonate, **1a** and (b) a 1:1 mixture with P=^{18}O isotopomer **1a** (^{18}O). (c) MI spectrum (2ffr, 8 keV) of the *m/z* 108 molecular ion of ethylene phosphonate, **1a**. The inset shows the partial spectrum of the *m/z* 110 ions of the P=^{18}O isotopomer **1a** (^{18}O).

an energetically much more favourable neutral, i.e., HO–P(=O)$_2$, metaphosphoric acid. The IE of C_2H_4 (10.51 eV [26]) is considerably lower than that of metaphosphoric acid (12.2 eV, Table 1b, this work), thus explaining why the complementary process to HO–P(=O)$_2^{\bullet+}$ (*m/z* 80) + C_2H_4 does not occur.

The formation of *m/z* 28 $C_2H_4^{\bullet+}$ ions also dominates the MI spectrum of the molecular ion, see Fig. 2c, but loss of CH_2O is now absent. Instead, peaks are observed at *m/z* 79 and 80 which correspond to the losses of HCO$^{\bullet}$ and CO, respectively. The product ions generated in these reactions are CH_3O–P–OH^+ and CH_3O–P(H)–$OH^{\bullet+}$, respectively (from a comparison of their CID spectra with the reference spectra of Ref. [13]). Both processes represent slow rearrangement reactions which do not feature in either the CID spectrum or the EI mass spectrum. This is also true for the prominent loss of HOPO which yields ions of *m/z* 44 whose structure was established as CH_2=CH–$OH^{\bullet+}$. The MI spectrum of the ^{18}O-labelled isotopologue, **1a**$^{\bullet+}$ (^{18}O), [–OCH_2CH_2O–]P(H)=^{18}O, inset Fig. 2c, reveals that, notably in the loss of HCO$^{\bullet}$ and the concomitant decarbonylation, all oxygen atoms have become equivalent, indicating that these slow dissociations are accompanied by extensive skeletal rearrangements via ring-opened structures. On the other hand, in the stable ions sampled by the CID experiment, the labelled O-atom retains its structural integrity: ions **1a**$^{\bullet+}$ (^{18}O) specifically lose CH_2O, see Fig. 3.

The kinetic energy release (KER) [27] values associated with most of the reactions displayed in the MI spectrum of Fig. 2c are unexceptional. However, the *m/z* 28 peak is characteristically narrow and the KER derived from its width at half-height, $T_{0.5}$, is $<$0.5 meV. Such small KER values often indicate that the rearrangement/dissociations reactions proceed via ion–dipole complexes. In contrast, the peak at *m/z* 80 is broad and associated with a large energy release, $T_{0.5}$ = 240 meV, indicating that the decarbonylation reaction is associated with a considerable reverse activation energy.

The ethylene phosphite tautomer **1b**$^{\bullet+}$ was generated via the following three routes described in Section 1. As mentioned ionized DMP readily isomerizes via a 1,4-H shift into its distonic counterpart CH_2O–$(CH_3O)P(H)OH^{\bullet+}$. This distonic ion serves as the immediate precursor for the abundant loss of CH_2=O that characterizes the EI spectrum of DMP. By analogy, it may be expected that the *m/z* 108 ions generated by loss of CH_2=O from ionized **III**—which form the base peak in its EI mass spectrum—are generated in the same way, producing the desired "enol" ion **1b**$^{\bullet+}$, see route (i) of Scheme 1.

However, formaldehyde loss from **III**$^{\bullet+}$ could also involve elimination of the –CH_2–O– moiety

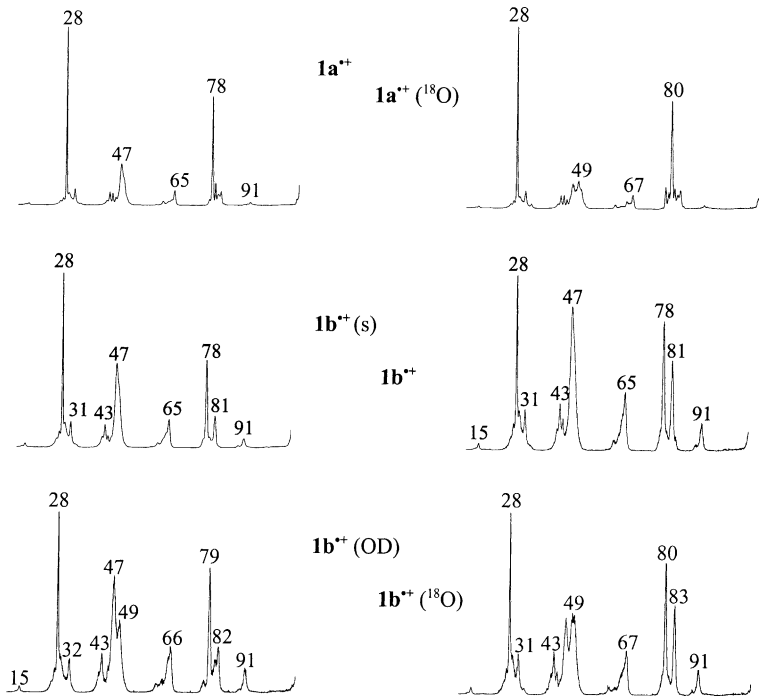

Fig. 3. CID mass spectra (3ffr) of ethylene phosphonate ions **1a**$^{\bullet+}$ and ethylene phosphite ions **1b**$^{\bullet+}$ and selected labelled isotopologues. Ions **1b**$^{\bullet+}$ (s) are source generated ions; all other enol type ions were "cold" ions generated by CID of the metastable precursor ions.

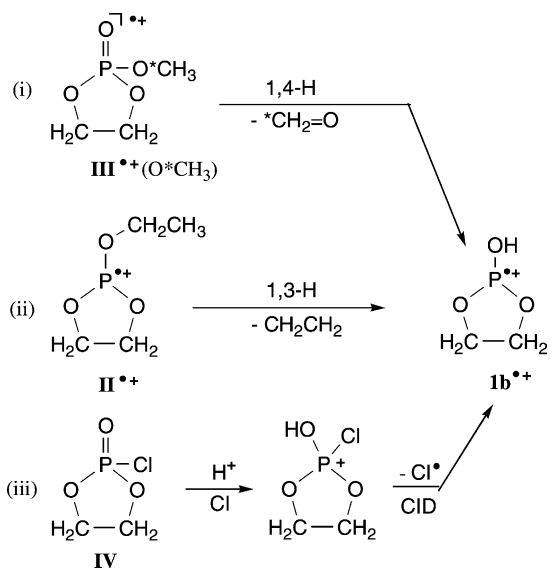

Scheme 1.

of the ring, to yield distonic ions of structure CH_2–O–P(=O)$OCH_3^{\bullet+}$ (ion **1g**$^{\bullet+}$ in Table 1a) instead. Examination of the spectra of labelled isotopologues revealed that the latter reaction does take place, albeit to a small extent: in their EI mass spectra **III** ($O^{13}CH_3$) and **III** (OCD_3) display losses of $^{13}CH_2O/CH_2O$ and CD_2O/CH_2O in a ratio of 10:1. We have therefore used these labelled isotopologues for the generation of ions of putative structure **1b**$^{\bullet+}$ and **1b**$^{\bullet+}$ (OD). In this context, we note that the MI spectrum of *m*/*z* 108 ions CH_2–O–P(=O)$OCH_3^{\bullet+}$ (**1g**$^{\bullet+}$) is dominated by loss of HCO$^{\bullet}$ yielding product ions of structure CH_3O–P–OH^+ (from a comparison of the CID spectrum with a reference CID spectrum obtained in the work of Ref. [13]). The HCO$^{\bullet}$ loss is highly specific: the isotopologues CH_2–O–P(=O)$O^{13}CH_3^{\bullet+}$ and CH_2–O–P(=O)$OCD_3^{\bullet+}$ exclusively lose HCO$^{\bullet}$.

The MI spectrum of source generated ions **1b**$^{\bullet+}$ from **III** ($O^{13}CH_3$) was obtained and the spectrum

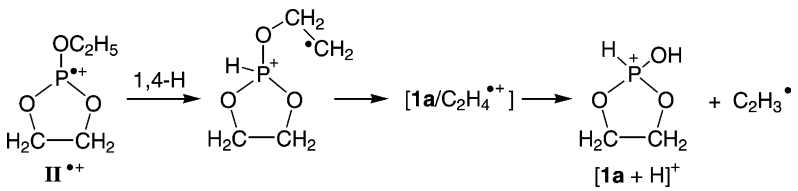

Scheme 2.

(not shown) appeared to be identical with that presented in Fig. 2c for ions $\mathbf{1a}^{\bullet+}$ generated from ethylene phosphonate. Similarly, the MI spectra of the *m*/*z* 109 ions $\mathbf{1b}^{\bullet+}$ (OD) generated from **III** (OCD_3) and $\mathbf{1a}^{\bullet+}$ (P–D) from P–D-labelled ethylene phosphonate were found to be identical.

In contrast, the CID spectrum of $\mathbf{1b}^{\bullet+}$ (see Fig. 3), is clearly and characteristically different from that of $\mathbf{1a}^{\bullet+}$. Upon collisional activation, ions $\mathbf{1b}^{\bullet+}$ uniquely lose $C_2H_3^{\bullet}$ and $OH^{\bullet}$, yielding *m*/*z* 81 $(HO)_2P{=}O^+$ ions and (cyclic) *m*/*z* 91 ions, respectively; the calculations indicate (see Table 1b and also Scheme 3), that these two dissociations have about the same minimum energy requirement.

The observation that the MI spectra of $\mathbf{1a}^{\bullet+}$ and $\mathbf{1b}^{\bullet+}$ are identical raises the possibility that the CID spectrum of source generated ions $\mathbf{1b}^{\bullet+}$ actually represents a mixture of ions $\mathbf{1b}^{\bullet+}$ and $\mathbf{1a}^{\bullet+}$ (and perhaps also of other isomers). To probe this possibility, we set out to generate ions $\mathbf{1b}^{\bullet+}$ at lower internal energies, where formation of the higher energy species $\mathbf{1a}^{\bullet+}$ cannot compete. One way to achieve this is to generate ions $\mathbf{1b}^{\bullet+}$ from *metastable* precursor ions. Unfortunately, compound **III** cannot be used for this purpose as the loss of $CH_2{=}O$ is an insignificant reaction of metastable ions $\mathbf{III}^{\bullet+}$. Rather these precursor ions dissociate almost exclusively, via a remarkable skeletal rearrangement, by loss of $C_3H_3^{\bullet}$ to yield *m*/*z* 99 H_4PO_4 ions, most likely protonated phosphoric acid.

Loss of C_2H_4 from ionized ethyl ethylene phosphite, $\mathbf{II}^{\bullet+}$, depicted as route (ii) in Scheme 1, proved to be a better choice for the generation of ions $\mathbf{1b}^{\bullet+}$ of low internal energy. The MI spectrum (and also the CID spectrum) of $\mathbf{II}^{\bullet+}$ is dominated by two competing processes, viz. loss of $C_2H_3^{\bullet}$ and C_2H_4 yielding peaks at *m*/*z* 109 and *m*/*z* 108 with an intensity ratio of 1.5. The loss of $C_2H_3^{\bullet}$ involves a double H-transfer and yields protonated ethylene phosphonate, $[\mathbf{1a}+H]^+$. A plausible mechanism for this reaction loss involves a 1,4-H shift to yield an intermediate ion that develops into an ion–dipole complex $[\mathbf{1a}/C_2H_4^{\bullet+}]$ from which $[\mathbf{1a}+H]^+$ is formed by a proton transfer (Scheme 2).

The minimum (thermochemical) energy requirement for the above reaction is 35 kcal/mol (from ΔH_f $\mathbf{II}^{\bullet+}$ = 28 kcal/mol, Table 1b, ΔH_f $[\mathbf{1a}+H]^+$ = −9 kcal/mol, Table 1b and ΔH_f $C_2H_3^{\bullet}$ = 72 kcal/mol [28]). In contrast, generation of $\mathbf{1a}^{\bullet+}$ by loss of C_2H_4 from either of the intermediate ions in Scheme 2 has a minimum energy requirement of 57 kcal/mol (from ΔH_f $\mathbf{1a}^{\bullet+}$ = 72 kcal/mol, Table 1b and ΔH_f C_2H_4 = 12.5 kcal/mol [26]), 22 kcal/mol higher than that calculated for the $C_2H_3^{\bullet}$ loss. Moreover, since IE(C_2H_4), 10.5 eV [26], is lower than that of **1a**, 10.7 eV (this work, Table 1b), dissociation into $C_2H_4^{\bullet+}$ + **1a** rather than C_2H_4 + $\mathbf{1a}^{\bullet+}$ is expected and this process is not observed. Thus, the competing loss of C_2H_4 observed in the MI spectrum of $\mathbf{II}^{\bullet+}$ does not yield "keto" ions $\mathbf{1a}^{\bullet+}$.

Another possibility, namely that the loss of C_2H_4 from metastable ions $\mathbf{II}^{\bullet+}$ involves a 1,5-H shift to generate the distonic isomer $\mathbf{1c}^{\bullet+}$ can also be discarded: the minimum energy requirement for this reaction is calculated to be 46 kcal/mol (using ΔH_f $\mathbf{1c}^{\bullet+}$ = 62 kcal/mol, Table 1a), i.e., some 11 kcal/mol higher than that calculated for the $C_2H_3^{\bullet}$ loss.

In contrast, the mechanism proposed in Scheme 1 for the loss of C_2H_4 from $\mathbf{II}^{\bullet+}$, a β-H transfer (1,3-H shift) to yield "enol" ions $\mathbf{1b}^{\bullet+}$, does account for the observed competition with $C_2H_3^{\bullet}$ loss. Its minimum energy requirement of 22 kcal/mol (from ΔH_f $\mathbf{1b}^{\bullet+}$ =

37 kcal/mol, Table 1b) is actually lower than that calculated for the loss of $C_2H_3^{\bullet}$. However, the 1,3-H shift associated with the C_2H_4 loss imposes a barrier, estimated to be 30–35 kcal/mol,[1] which is expected to be higher than the 1,4-H shift/H^+ transfer associated with the $C_2H_3^{\bullet}$ loss. This makes the two reactions energetically equivalent and accounts for the observation that they are both prominently observed in the MI spectrum of **II**$^{\bullet+}$.

Thus, there is little doubt that *metastable* ions **II**$^{\bullet+}$ exclusively generate "cold" enol ions **1b**$^{\bullet+}$ and this is borne out by its CID spectrum which is shown in Fig. 3. The spectrum is similar to that of the source generated ions but the structure diagnostic peaks of the enol ions **1b**$^{\bullet+}$ at *m/z* 91 and *m/z* 81 are more prominent.

Finally, we have explored yet another route to confirm the CID characteristics of ions **1b**$^{\bullet+}$. Protonation of **IV** under conditions of chemical ionization, route (iii) in Scheme 1, followed by collision-induced loss of $Cl^{\bullet}$ of the protonated molecule in the 2ffr yields *m/z* 108 ions whose 3ffr CID spectrum is closely similar to that observed for the "cold" ions **1b**$^{\bullet+}$ generated by the dissociative ionization route (ii). The same obtains for ions **1b**$^{\bullet+}$ (OD) generated by the deuteronation of **IV** using $CD_3C(=O)CD_3$ as the reactant.

The NR mass spectra of **1a**$^{\bullet+}$ and **1b**$^{\bullet+}$ are given in Fig. 4. Both spectra are very different from their respective CID spectra: the base peaks in both NR spectra are at *m/z* 47, $P{=}O^+$. This peak we propose, as well as that at *m/z* 63 which is not present in the CID spectra, arise from dissociations of the *m/z* 80 ions, $HOPO_2^{\bullet+}$ (which cleanly shifts to *m/z* 82 and *m/z* 79 in the NR spectra of **1a**$^{\bullet+}$ (^{18}O) and **1a**$^{\bullet+}$ (P–D)) formed by collisional ionization of the $HOPO_2$ molecules formed from the metastable ions: **1a**$^{\bullet+}$/**1b**$^{\bullet+}$ → $C_2H_4^{\bullet+} + HOPO_2$, $HOPO_2 \rightarrow HOPO_2^{\bullet+} \rightarrow PO_2^{\bullet+} \rightarrow PO^{\bullet+}$. It can also be seen

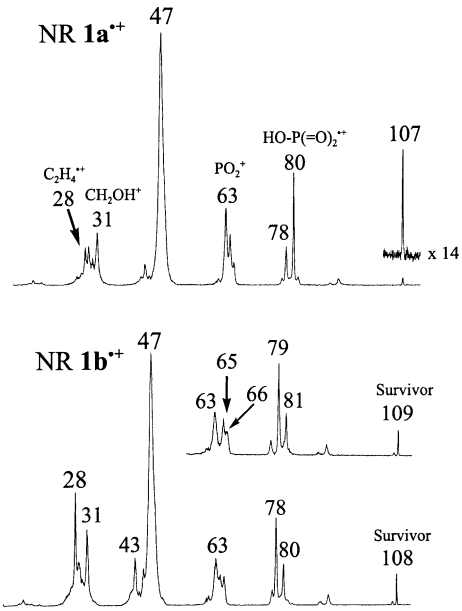

Fig. 4. Eight keV NRMS of ions **1a**$^{\bullet+}$ and **1b**$^{\bullet+}$. The inset shows the partial NR spectrum of **1b**$^{\bullet+}$ (OD).

that no survival ion signal is present for the keto ions, whereas such a signal is clearly present for the enol ions. The more extensive dissociation of **1a**$^{\bullet+}$ upon NR (as compared to EI or CID) indicates that NR deposits higher average internal energies than EI or CID [29]. It is also of interest to note that *m/z* 78, $CH_2O{-}P{-}OH^{\bullet+}$, is more intense in the NR spectrum of **1b**$^{\bullet+}$ and that only ions **1b**$^{\bullet+}$ can form *m/z* 78 without rearrangement. Thus, the enol ions (at least in part) survive the NR experiment, but the keto ions do not. We take this finding as showing that the enol ions lie in a much deeper well than the keto ions, see Scheme 3.

From the above we conclude the following: the ethylene phosphonate and ethylene phosphite ions (**1a**$^{\bullet+}$ and **1b**$^{\bullet+}$, respectively) can be independently generated and identified in the gas-phase. The non-dissociating ions do not interconvert to a significant extent. However, metastable ions **1a**$^{\bullet+}$ and **1b**$^{\bullet+}$ do interconvert leading to a common dissociation channel, i.e., that leading to $C_2H_4^{\bullet+} + HOPO_2$ having the same kinetic energy release. Competing fragmentations include the losses of CO and

[1] The thermochemical energy requirement for the reaction $CH_2{=}CH{-}OC_2H_5^{\bullet+} \rightarrow CH_2{=}CH{-}OH^{\bullet+} + C_2H_4$ is 25 kcal/mol [25], 8 kcal/mol lower than the experimentally observed value of 33 kcal/mol (J.L. Holmes, J.K. Terlouw, F.P. Lossing, J. Phys. Chem. 80 (1976) 2860). The latter value is most readily attributed to the barrier for 1,3-H shift in this dissociation.

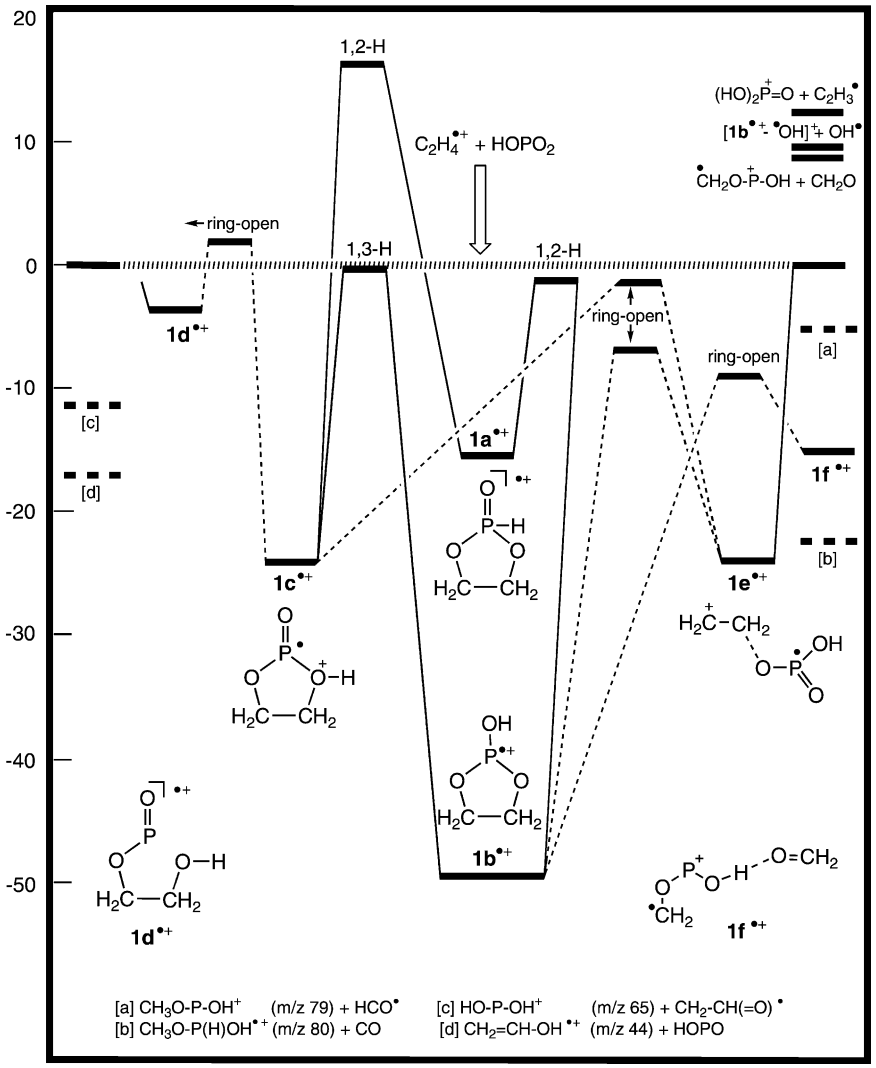

Scheme 3. Potential energy diagram describing the isomerization and dissociation chemistry of the ethylene phosphonate ion $\mathbf{1a}^{\bullet+}$, derived from CBS-QB3 calculations (298 K, Table 1a). All energies, in kcal/mol, are relative to the dissociation level $C_2H_4^{\bullet+} + HOPO_2$.

$HCO^{\bullet}$ and ^{18}O-labelling experiments indicate that in these fragmentations all oxygen atoms become positionally equivalent. It is therefore highly likely that such equilibration reactions also occur for the dominant metastable reaction, viz. formation of $C_2H_4^{\bullet+} + HOPO_2$. In the following we shall use results from our ab initio calculations to rationalize the above experimental observations.

3.2. The isomerization and dissociation behaviour of ethylene phosphonate/phosphite ions

In our analysis of the experimental and theoretical results we will use the energy diagram of Scheme 3 as our starting point. This diagram summarizes the CBS-QB3 (298 K) computational results on the various isomerization routes for ions $\mathbf{1a}^{\bullet+}$ and $\mathbf{1b}^{\bullet+}$ and

their low energy dissociation by loss of HO–P(=O)$_2$. The geometries of the species encountered are given in Fig. 1.

First it can be seen, in agreement with experiment, that ions **1b**$^{\bullet+}$ are thermodynamically more stable than **1a**$^{\bullet+}$ and that they lie in a deep potential well. This explains the observed survivor signal in the NR mass spectrum of **1b**$^{\bullet+}$. Just below the metastable dissociation level, see the dashed line in Scheme 3, ions **1a**$^{\bullet+}$ can undergo a 1,2-H shift to produce the very stable enol ion **1b**$^{\bullet+}$. It is found that these ions can undergo ring-opening below the metastable window to produce ions **1e**$^{\bullet+}$. The latter ions, see Fig. 1 which depicts two configurations of closely similar energy labelled as **1e**$^{\bullet+}$ (α) and **1e**$^{\bullet+}$ (β), contain a long O···C bond and are more accurately described as an ion–dipole complex between $C_2H_4^{\bullet+}$ and $HOPO_2$. This complex is the reacting configuration for formation of $C_2H_4^{\bullet+}$ from both **1a**$^{\bullet+}$ and **1b**$^{\bullet+}$. The small kinetic energy release associated with this dissociation is attributed to the large density of states of such ion–dipole complexes [30]. It is also found that, again just below the metastable window, ions **1b**$^{\bullet+}$ can rearrange by way of a 1,3-H shift to the distonic isomer **1c**$^{\bullet+}$. This species is unattainable directly from **1a**$^{\bullet+}$ as the calculated barrier for this 1,2-H shift lies very high, see Scheme 3. However, ions **1a**$^{\bullet+}$ can isomerize into the distonic ion via the enol ion **1b**$^{\bullet+}$. The distonic ion **1c**$^{\bullet+}$ may undergo ring-opening to ion **1d**$^{\bullet+}$ and the latter ion may be responsible for some of the other (minor) processes observed for the metastable ions (such as *m*/*z* 44, CH_2=CH–OH$^{\bullet+}$) but these matters were not further investigated. However, the transition state for this ring-opening lies slightly above the threshold for dissociation into $C_2H_4^{\bullet+}$ and $HOPO_2$.

An important reaction upon collisional activation of both ions **1a**$^{\bullet+}$ and **1b**$^{\bullet+}$ is the formation of $^{\bullet}CH_2$–O–P$^+$–OH + CH_2O, see Fig. 3. From NR data we had tentatively concluded that ions **1b**$^{\bullet+}$ could lead to these products. Indeed, according to our ab initio calculations ions **1b**$^{\bullet+}$ can undergo, below the dissociation threshold for loss of HO–P(=O)$_2$, C–C ring-opening to produce the ion–dipole complex $^{\bullet}CH_2$–O–P$^+$–OH···O=CH_2, **1f**$^{\bullet+}$ which then dissociates. Ion **1f**$^{\bullet+}$ may also be the reacting configuration for the observed (minor) losses of HCO$^{\bullet}$ and CO.

We conclude from our calculations that ions **1a**$^{\bullet+}$, **1b**$^{\bullet+}$ and **1c**$^{\bullet+}$ (and perhaps also **1e**$^{\bullet+}$ and **1f**$^{\bullet+}$) may more or less freely interconvert prior to dissociation. Nevertheless, this interconversion cannot rationalize the observation that the oxygen atoms become positionally equivalent. However, according to our calculations the distonic ion, **1c**$^{\bullet+}$, can undergo an O–C ring-opening to produce the ion–dipole complex **1e**$^{\bullet+}$ which can also be formed from the enol ion **1b**$^{\bullet+}$. The (inter)conversion **1a**$^{\bullet+}$ → **1b**$^{\bullet+}$ → **1e**$^{\bullet+}$ → **1c**$^{\bullet+}$ → **1b**$^{\bullet+}$ → **1a**$^{\bullet+}$ rationalizes the observed "scrambling" of the oxygen atoms in ions **1a**$^{\bullet+}$ and **1b**$^{\bullet+}$.

3.3. The benzonitrile-assisted tautomerization of ethylene phosphonate

If we wish to catalyze, by proton-transport catalysis, a 1,2-H shift, then a suitable base should fulfil several criteria [15e], the most important one being the proton affinity (PA) criterion. Following Scheme 3, if we wish to successfully isomerize **1a**$^{\bullet+}$ to **1b**$^{\bullet+}$ then the PA of the base should lie between the PA of the [**1a** − H]$^{\bullet}$ radical at P and O. From the energy of [**1a** − H]$^{\bullet}$ in Table 1b and the energies of **1a**$^{\bullet+}$ and **1b**$^{\bullet+}$ we may evaluate these PAs: PA [**1a** − H]$^{\bullet}$ at P = 159 kcal/mol and PA [**1a** − H]$^{\bullet}$ at O = 194 kcal/mol. Therefore, benzonitrile having a PA of 194 kcal/mol [26] is a suitable candidate to catalyze the above 1,2-H shift.

Benzonitrile was admitted at an indicated pressure of 6×10^{-5} to the ion source and a small amount of **1a** was introduced into the ion source. The complex [**1a**···BN]$^{\bullet+}$ thus formed, see Fig. 5 was selectively transmitted into the second ffr. This complex dissociates spontaneously to *m*/*z* 108 and BN, together with some other minor fragments, see Fig. 5. The ions with *m*/*z* 108 were transmitted to the third ffr where they were collisionally probed; the resulting CID mass spectrum is also given in Fig. 5. Comparison of this spectrum with those of Fig. 3 leaves no doubt that the initial keto ions **1a**$^{\bullet+}$ have completely rearranged to the enol ions **1b**$^{\bullet+}$ under the influence of benzonitrile.

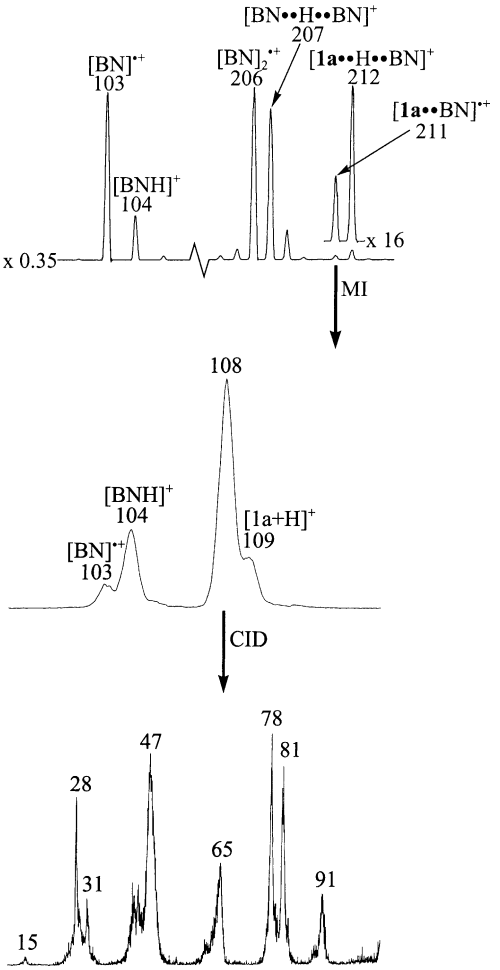

Fig. 5. CID mass spectrum of the *m/z* 108 ions **1b**$^{\bullet+}$ generated from metastable ethylene phosphonate/benzonitrile complex ions [**1a**···BN]$^{\bullet+}$.

Two different mechanisms may operate for the benzonitrile-assisted tautomerization of **1a**$^{\bullet+}$. The first mechanism involves a true proton-transport catalysis in which the P–H proton of *ionized* **1a**$^{\bullet+}$ is donated to benzonitrile and the same proton is then donated back to the oxygen atom. In the second mechanism, it is benzonitrile which is ionized and which donates the proton to the P=O oxygen atom of *neutral* **1a**. Next the P–H proton is donated to the benzonitrile radical. This mechanism is termed a "quid-pro-quo" mechanism and is depicted in Scheme 4. Labelling can differentiate the two mechanisms: using benzonitrile-d_5 the rearranged enol will appear at *m/z* 108 if the isomerization is a true proton-transport catalysis; however for a "quid-pro-quo" mechanism the rearranged enol will appear at *m/z* 109, see Scheme 4.

Using benzonitrile-d_5 as the solvent molecule, the reaction in the *m/z* 216 encounter complex [**1a**···BN-d_5]$^{\bullet+}$ commences with a D^+ transfer. The next step involves a back-transfer of a $H^\bullet$ radical to the phenyl ring of BN, yielding the hydrogen bridged radical cation (HBRC) [**1b**$^{\bullet+}$(OD)···BN-d_4] which, either spontaneously or by collisional activation, dissociates into "enol" ions **1b**$^{\bullet+}$ (OD) at *m/z* 109. If a proton-transport type mechanism were operative, the final complex would be a HBRC of the composition [**1b**$^{\bullet+}$(OH)···BN-d_5] which would decompose into "enol" ions **1b**$^{\bullet+}$ (OH) at *m/z* 108.

Unfortunately, the experimental verification of the above proposal is complicated by the fact that the molecular mass of benzonitrile-d_5 is the same as that of **1a**. From Fig. 5 (top spectrum), it follows that in the CI experiment with unlabelled benzonitrile, [BN···BN]$^{\bullet+}$ dimer ions are formed which are ca. 30 times more abundant than the mixed dimer ions [**1a**···BN]$^{\bullet+}$. Therefore, the *m/z* 216 peak in the CI experiment of **1a** with BN-d_5 is dominated by isobaric [BN-d_5]$_2^{\bullet+}$ ions, whose MI spectrum is characterized by a single peak at *m/z* 108, [BN-d_5]$^{\bullet+}$. Moreover, the benzonitrile-d_5 used contained ca. 5% of the d_4-isotopologue and since, see Fig. 5 (top spectrum) proton-bound dimer ions [BN···H···BN]$^+$ are also abundantly generated in the CI experiment, the *m/z* 216 ions will also contain interfering ions of structure [BN-d_5···H···BN-d_4]$^+$. The MI spectrum of [BN···H···BN]$^+$ shows a single peak at *m/z* 104, BNH^+, and by analogy [BN-d_5···H···BN-d_4]$^+$ is expected to yield peaks at both *m/z* 108 [BN-d_4H]$^+$ and *m/z* 109 [BN-d_5H]$^+$. Finally, the MI spectrum of unlabelled ions [**1a**···BN]$^{\bullet+}$, see Fig. 5 (middle spectrum), also contains a peak at *m/z* 104, BNH^+, which will shift to *m/z* 109 in the MI spectrum of [**1a**···BN-d_5]$^{\bullet+}$.

Thus, the MI spectrum of the *m/z* 216 ions formed in the CI experiment of **1a** with BN-d_5, which

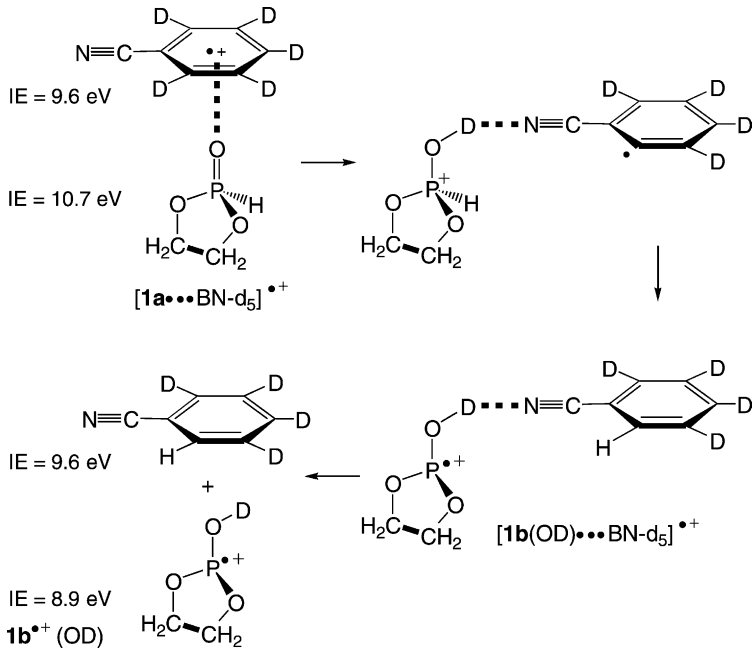

Scheme 4.

displays prominent peaks at *m*/*z* 108 and *m*/*z* 109 (in a 3:1 intensity ratio) cannot be used to decide between the proposed "quid-pro-quo" tautomerization mechanism and proton-transport catalysis. However, examination of the CID spectra of the *m*/*z* 108 and *m*/*z* 109 ions of the *m*/*z* 216 MI spectrum does allow differentiation: the CID spectrum of the *m*/*z* 108 ions is identical with that of *m*/*z* 108 ions independently generated from $[BN\text{-}d_5]_2^{\bullet+}$. The spectrum, even when recorded at a 10× higher amplification, does not show a detectable signal at *m*/*z* 47. Since this peak (PO^+) is uniquely characteristic for the presence of phosphorus containing ions, we conclude that *m*/*z* 108 ions $\mathbf{1b}^{\bullet+}$ (OH) are *not* formed. This effectively rules out the proton-transport catalysis mechanism.

The CID spectrum of the *m*/*z* 109 ions is shown in Fig. 6. Although this spectrum is dominated by ions generated from the decomposition of protonated BN-d_5, as evidenced by the base peak at *m*/*z* 81 (loss of DCN) and the peaks at *m*/*z* 65/66 and 52/54, the spectrum also contains a narrow peak at *m*/*z* 28 and the

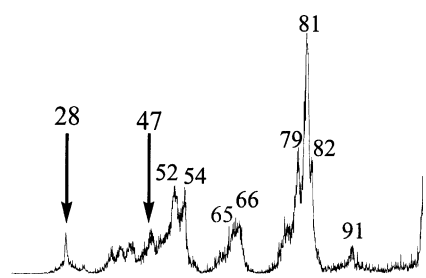

Fig. 6. CID mass spectrum (3ffr) of the *m*/*z* 109 ions in the MI spectrum (2ffr) of the *m*/*z* 216 ions generated from ethylene phosphonate and benzonitrile-d_5 under chemical ionization conditions.

tell-tale peak at *m*/*z* 47, indicative of the presence of phosphorus containing ions. Although the $[BN\text{-}d_5H]^+$ interference does not allow us to firmly conclude that "enol" ions $\mathbf{1b}^{\bullet+}$ (OD) are generated in the experiment with benzonitrile-d_5, there is little doubt that a H/D exchange in the encounter complex as dictated by the "quid-pro-quo" mechanism is indeed operative.

From a theoretical point of view, the proton-transport catalysis mechanism is also unlikely since IE (BN) (9.6 eV, Ref. [26]) is so much lower than

IE (**1a**) (10.7 eV). As a consequence the charge in the [**1a**···BN]$^{\bullet+}$ complex will be located on the BN moiety, thus prohibiting the first step in the proton-transport catalysis mechanism, i.e., the proton abstraction from **1a**$^{\bullet+}$. However, the same IE difference favours the "quid-pro-quo" mechanism in the following way. An estimate of the relative energies along this pathway may be obtained by combining empirical data with the results given in Table 1b, together with computational results obtained previously for the acetamide/BN system [17].

The reaction sequence is given by: [**1a**$^{\bullet+}$ + BN] → [**1a** + BN$^{\bullet+}$] → [**1a**···BN$^{\bullet+}$] → TS1 → [**1a**H$^+$···(BN–H)$^\bullet$] → TS2 → [**1b**$^{\bullet+}$···BN]$^\bullet$ → [**1b**$^{\bullet+}$ + BN].

With [**1a**$^{\bullet+}$ + BN] as the reference level, and stabilization energies (SE) [31] for the complexes derived from the empirical relationship SE = 30–0.25|ΔPA|, we find E_{rel} values of −24, −51 and −64 kcal/mol for [**1a** + BN$^{\bullet+}$], [**1a**H$^+$···(BN-H)$^\bullet$] and [**1b**$^{\bullet+}$···BN], respectively (using ΔH_f (BN$^{\bullet+}$) = 274 kcal/mol, ΔH_f ([BN − H]$^\bullet$) = 111 kcal/mol [17], PA([**1a**/**1b** − H]$^\bullet$) at O = 194 kcal/mol, PA(**1a**) = 200 kcal/mol (Table 1b), PA([BN − H]$^\bullet$) = 204 kcal/mol [17]). For the complex [**1a**···BN$^{\bullet+}$], E_{rel} is estimated as −36 kcal/mol, using the SE (12 kcal/mol) calculated for the [acetamide···BN$^{\bullet+}$] complex [17]. If we further assume that the heights of the isomerization barriers represented by TS1 and TS2 are comparable in magnitude to those calculated for the acetamide/BN system [17], these TSs will lie at about the same energy level as that for [**1a** + BN$^{\bullet+}$]. In our experiments, internal energies up to the [**1a**$^{\bullet+}$ + BN] level of energy may well be available to the reactants, thereby providing sufficient energy for the isomerization reaction [**1a**···BN]$^{\bullet+}$ → [**1b**···BN]$^{\bullet+}$ to proceed. The observation, see Fig. 5, that the resulting [**1b**···BN]$^{\bullet+}$ complex also dissociates into BNH$^+$ (m/z 104) + [**1b** − H]$^\bullet$ supports the computational finding that the PA of [**1a**/**1b** − H]$^\bullet$ at O is closely similar to that of BN (194 kcal/mol, see above).

In summary, theory and experiment yield a consistent potential energy profile for the cyclic phosphonate/phosphite system showing that non-dissociating ions **1a**$^{\bullet+}$ retain their structure identity in the microsecond time-frame. However, the interaction of **1a** with a BN molecule in a chemical ionization type experiment readily yields the more stable "enol" type ion **1b**$^{\bullet+}$. Experiments with benzonitrile-d_5 support the proposal that this interaction does not involve the lowering of the 1,2-H shift barrier between the tautomers via a proton-transport catalysis type mechanism. Rather, a "quid-pro-quo" mechanism is operative, analogous to that proposed for the benzonitrile-assisted enolization of acetamide [17]. In this mechanism, the ionized benzonitrile component of the encounter complex [**1a**···BN]$^{\bullet+}$ donates a proton to the O-atom of the phosphonate's O=P(H) functionality. This is followed by a back-transfer of the P–H hydrogen atom to benzonitrile's phenyl ring, yielding a H-bridged radical cation of the type $C_6H_5C{\equiv}N\cdots H{-}O{-}P[{-}OCH_2CH_2O{-}]^{\bullet+}$. This ion serves as the immediate precursor in the formation of the ethylene phosphite ion, **1b**$^{\bullet+}$, and benzonitrile.

Acknowledgements

J.K.T. thanks the Natural Sciences and Engineering Research Council of Canada (NSERC) for continuing financial support. L.N.H. thanks McMaster University for the Sherman Award. P.J.A.R. thanks The Netherlands Organization for Scientific Research (NWO) for making available the SGI TERAS computer of SARA (Amsterdam). The contribution of Cathy Wong to the experimental work of this study is gratefully acknowledged.

References

[1] D.E.C. Corbridge, Phosphorus: An Outline of Its Chemistry, Biochemistry, and Uses, 5th ed., Elsevier, New York, 1995.
[2] J. Emsley, D. Hall, The Chemistry of Phosphorus, Harper and Row Ltd., London, 1976.
[3] M. Eto, Organophosphorus Pesticides: Organic and Biological Chemistry, CRC Press, Cleveland, OH, 1974.
[4] (a) R.A.J. O'Hair, in: F.R. Hartley (Ed.), The Chemistry of Organophosphorus Compounds, vol. 4, Chapter 8, Wiley, London, 1996;
(b) R.G. Gillis, J.L. Occolowitz, in: M. Halmann

(Ed.), Mass Spectrometry of Phosphorus Compounds in Analytical Chemistry of Phosphorus Compounds, Chapter 8, Wiley/Interscience, New York, 1972;
(c) J.R. Chapman, Organophosphorus Chem. 14 (1983) 278;
(d) J. Granoth, Top. Phosphorus Chem. 8 (1976) 41.
[5] (a) S. Gevrey, A. Luna, M.-H. Taphanel, J. Tortajada, J.-P. Morizur, Int. J. Mass Spectrom. 195/196 (2000) 545;
(b) J.-F. Gal, M. Herreros, P.C. Maria, L. Operti, C. Pettigiani, R. Rabezanna, G.A. Vaglio, J. Mass Spectrom. 34 (1999) 1296;
(c) B.L.M. van Baar, A.G. Hulst, E.R.J. Wils, J. Mass Spectrom. 32 (1998) 1104.
[6] (a) J.L. Occolowitz, G.L. White, Anal. Chem. 35 (1963) 1179;
(b) J.G. Pritchard, Org. Mass Spectrom. 3 (1970) 163;
(c) E. Santoro, Org. Mass Spectrom. 7 (1973) 589;
(d) D.A. Bafus, E.J. Gallegos, R.W. Kiser, J. Phys. Chem. 70 (1966) 2614;
(e) J. Fischler, M. Halman, J. Chem. Soc. (1964) 31.
[7] (a) Tandem Mass Spectrometry, F.W. McLafferty (Ed.), Wiley, New York, 1983;
(b) K. Levsen, H. Schwarz, Mass Spectrom. Rev. 2 (1983) 77.
[8] K.L. Busch, G.L. Glish, S.A. McLuckey, Mass Spectrometry/Mass Spectrometry, VCH, New York, 1988.
[9] J.L. Holmes, Org. Mass Spectrom. 20 (1985) 169.
[10] (a) H.I. Kenttämaa, R.G. Cooks, J. Am. Chem. Soc. 107 (1985) 1881;
(b) J.S. Brodbelt, H.I. Kenttämaa, R.G. Cooks, Org. Mass Spectrom. 23 (1988) 6;
(c) L. Zeller, J. Farrell Jr., P. Vainiotalo, H.I. Kenttämaa, J. Am. Chem. Soc. 114 (1992) 1205;
(d) K.M. Stirk, P. Lin, T.D. Ranatunga, L.C. Zeller, J.T. Farrell Jr., H.I. Kenttämaa, Int. J. Mass Spectrom. Ion Process. 130 (1994) 187.
[11] (a) J.R. Holtzclaw, J.R. Wyatt, J.E. Campana, Org. Mass Spectrom. 20 (1985) 90;
(b) J.R. Holtzclaw, J.R. Wyatt, Org. Mass Spectrom. 23 (1988) 261.
[12] F. Tureček, M. Gu, C.E.C.A. Hop, J. Phys. Chem. 99 (1995) 2278.
[13] L.N. Heydorn, Y. Ling, G. de Oliveira, J.M.L. Martin, C. Lifshitz, J.K. Terlouw, Zeitschrift für Physikalische Chemie 215 (2001) 141.
[14] Z. Rappoport (Ed.), The Chemistry of Enols, Wiley, New York, 1990.
[15] (a) D.K. Böhme, Int. J. Mass Spectrom. Ion Process. 115 (1992) 95;
(b) J.W. Gauld, H.-E. Audier, J. Fossey, L. Radom, J. Am. Chem. Soc. 118 (1996) 6299;
(c) J.W. Gauld, L. Radom, J. Am. Chem. Soc. 119 (1997) 9831;
(d) A.J. Chalk, L. Radom, J. Am. Chem. Soc. 119 (1997) 7573;
(e) A.J. Chalk, L. Radom, J. Am. Chem. Soc. 121 (1999) 1574;
(g) J. Chamot-Rooke, G. van der Rest, P. Mourgues, H.-E. Audier, Int. J. Mass Spectrom. 195/196 (2000) 385;
(g) M.A. Trikoupis, D.J. Lavarato, J.K. Terlouw, P.J.A. Ruttink, P.C. Burgers, European Mass Spectrom. 5 (1999) 431.
[16] (a) M.A. Trikoupis, J.K. Terlouw, P.C. Burgers, J. Am. Chem. Soc. 120 (1998) 12131;
(b) P. Mourgues, J. Chamot-Rooke, G. van der Rest, H. Nedev, H.E. Audier, T.B. McMahon, Int. J. Mass Spectrom. 210/211 (2001) 429;
(c) M.A. Trikoupis, P.C. Burgers, P.J.A. Ruttink, J.K. Terlouw, Int. J. Mass Spectrom. 217 (2002) 97.
[17] M.A. Trikoupis, P.C. Burgers, P.J.A. Ruttink, J.K. Terlouw, Int. J. Mass Spectrom. 210/211 (2001) 489.
[18] (a) A. Oswald, Can. J. Chem. 37 (1959) 1498;
(b) J. Cason, W.N. Baxter, W. DeAcetis, J. Org. Chem. 24 (1959) 247;
(c) K. Dimroth, R. Ploch, Chem. Ber. 90 (1957) 801.
[19] S.D. Taylor, R. Klugger, J. Am. Chem. Soc. 114 (1992) 3067.
[20] H.F. van Garderen, P.J.A. Ruttink, P.C. Burgers, G.A. McGibbon, J.K. Terlouw, Int. J. Mass Spectrom. Ion Process. 121 (1992) 159.
[21] G. Schalley, G. Hornung, D. Schröder, H. Schwarz, Chem. Soc. Rev. 27 (1998) 91.
[22] M.J. Frisch, G.W. Trucks, H.B. Schlegel, G.E. Scuseria, M.A. Robb, J.R. Cheeseman, V.G. Zakrzewski, J.A. Montgomery, R.E. Stratmann, J.C. Burant, S. Dapprich, J.M. Millam, A.D. Daniels, K.N. Kudin, M.C. Strain, O. Farkas, J. Tomasi, V. Barone, M. Cossi, R. Cammi, B. Mennucci, C. Pomelli, C. Adamo, S. Clifford, J. Ochterski, G.A. Petersson, P.Y. Ayala, Q. Cui, K. Morokuma, D.K. Malick, A.D. Rabuck, K. Raghavachari, J.B. Foresman, J. Cioslowski, J.V. Ortiz, B.B. Stefanov, G. Liu, A. Liashenko, P. Piskorz, I. Komaromi, R.L. Martin, D.J. Fox, T. Keith, M.A. Al-Laham, C.Y. Peng, A. Nanayakkara, R. Gomperts, C. Gonzalez, M. Challacombe, P.M.W. Gill, B.G. Johnson, W. Chen, M.W. Wong, J.L. Andres, M. Head-Gordon, E.S. Replogle, J.A. Pople, Gaussian 98, Revision A.9, Gaussian, Inc., Pittsburgh, PA, 1998.
[23] (a) M. Dupuis, D. Spangler, J. Wendolowski, NRCC Software Catalogue 1 Program No. QG01, GAMESS, 1980;
(b) M. Guest, J. Kendrick, GAMESS User Manual, An Introductory Guide, CCP/86/1, Daresbury Laboratories, 1986.
[24] (a) J.A. Montgomery Jr., M.J. Frisch, J.W. Ochterski, G.A. Petersson, J. Chem. Phys. 110 (1999) 2822;
(b) J.A. Montgomery Jr., M.J. Frisch, J.W. Ochterski, G.A. Petersson, J. Chem. Phys. 112 (2000) 6532.
[25] L.N. Heydorn, C.Y. Wong, R. Shrinivas, J.K. Terlouw, Int. J. Mass Spectrom. 225 (2003) 11.
[26] S.G. Lias, J.E. Bartmess, J.F. Liebman, J.L. Holmes, R.D. Levin, W.G. Mallard, J. Phys. Chem. Ref. Data 17 (Suppl. 1) (1988);
See also NIST Chemistry WebBook, http://webbook.nist.gov/chemistry/.
[27] J.L. Holmes, J.K. Terlouw, Org. Mass Spectrom. 15 (1980) 383.
[28] M.N. Glukhovtsev, R.D. Bach, Chem. Phys. Lett. 286 (1998) 51.
[29] S. Beranová, C. Wesdemiotis, J. Am. Chem. Soc. Mass Spectrom. 5 (1994) 1093.
[30] P.J.A. Ruttink, J. Phys. Chem. 91 (1987) 703.
[31] M. Meot-Ner (Mautner), J. Am. Chem. Soc. 106 (1984) 1257.